Canadian Chemical Transactions

ISSN 2291-6458 (Print), ISSN 2291-6466 (Online)
Year 2013 | Volume 1 | Issue 4 | Page 277-291

Research Article

DOI:10.13179/canchemtrans.2013.01.04.0041

Chelation Behavior of bis(1-(Pyridin-2-yl)ethylidene)-malonohydrazide towards Some Transition Metal Ions

Ola A. El-Gammal[1], Faten E. El-Morsy[1], Bakir Jeragh[2] and Ahmed A. El-Asmy[1,2]*

[1]*Department of Chemistry, Faculty of Science, Mansoura University, Mansoura, Egypt*

[2]*Department of Chemistry, Faculty of Science, Kuwait University, Kuwait*

** Corresponding Author: E-mail: aelasmy@ yahoo.com, Phone: 0096566734989*

Received: *September 23, 2013* ***Revised:*** *October 7, 2013* ***Accepted:*** *October 10, 2013* ***Published:*** *October18, 2013*

Abstract: Cr^{+3}, Mn^{+2}, Fe^{+3}, Co^{+2}, Ni^{+2}, Cu^{+2}, Cd^{+2}, VO^{+2} and Ag^{+} complexes of N^1, N^3-bis(1-(pyridin-2-yl)ethylidene)malonohydrazide (H_2L) have been prepared and spectroscopically characterized. The analytical and physical data support the formulae: $[Cu(H_2L)(OAc)_2].H_2O$; $[Co_2(L)(OAc)_2(H_2O)_2].H_2O$; $[Ni(H_2L)(OAc)_2.H_2O].H_2O$; $[Ag(H_2L)NO_3].EtOH$; $[Cd(H_2L)(OAc)_2].2H_2O$; $[(VO)_2(L)(OH)_2].H_2O$; $[Mn(H_2L)(H_2O)Cl_2].2H_2O$; $[Cr(H_2L)Cl_3].2H_2O$ and $[Fe(HL)(H_2O)Cl_2]$. The complexes are stable in air and insoluble in most common organic solvents but soluble in DMF and DMSO except for the Ag^{+} and Ni^{+2} complexes which are partially soluble. Different modes of chelation have been suggested for the ligand: neutral (bidentate or tridentate); monobasic (tridentate or tetradentate) and binegative hexadentate and supported by ^{1}HNMR for the diamagnetic complexes. All complexes have octahedral structure except for VO^{2+} complex which has a square-pyramid and intense color (green to brown). The TGA shows a high stability for some complexes in agreement with the high melting points. A variation in the overall scavenging ability was observed among the ligand and its metal complexes.

Keywords: Hydrazide; Spectra; Molecular Modeling; Superoxide Dismutase

1. INTRODUCTION

Many physiologically active hydrazides and hydrazones find applications in the treatment of diseases like tuberculosis, leprosy and mental disorders. They also act as herbicides, insecticides, nematocides, rodenticides and plant growth regulators [1-4] and Lakshmi Narayana Suvarapu find wide application for selective separation of metal ions [5-7]. Moreover, they were used for the spectrophotometric microdetermination of some metal ions and in polymer industry [8-10]. Schiff base hydrazone of pyridoxal phosphate and its analogous have been studied to understand the mechanism of action for vitamin B_6 containing enzymes [10]. A series of pyridazinyl hydrazones were found to inhibit *tyrosine* hydroxylase and *dopamine*- hydroxylase *in vivo* and *in vitro* [11]. Tridentate hydrazones have

ISSN 2291-6458 (Print), ISSN 2291-6466 (Online)
Year 2013 | Volume 1 | Issue 4 | Page 277-291

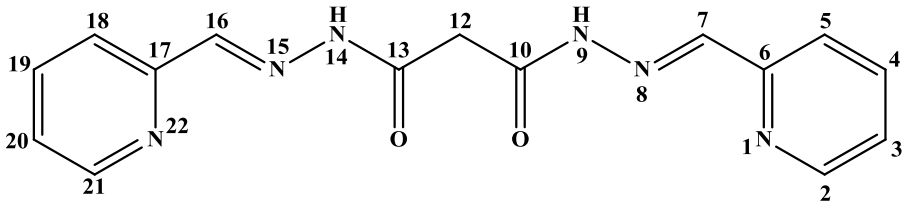

Structure 1. Numbering of the atoms in the ligand

been evaluated as potential oral iron-chelating drugs for genetic disorders such as thalassemia [12]. Salicylaldehydeacetyl hydrazone has also a potential biological activity and displayed radiation protective properties [13]. Hydrazones exhibit keto-enol tautomerism and can coordinate in neutral [14], monoanionic [15], dianionic [16-18] or tetraanionic form bearing unusual coordination numbers [16] in some mononuclear or binuclear species depending on the metal ion, its concentration, pH and the nature of the hydrazone. Isonicotinoylhydrazones act as good analytical reagents, but they have not been fully exploited. Hence, in the present investigation a detailed study of these reagents has been made with a view to find out their potentialities in inorganic analysis [19]. The octahedral Cu(II) complex with two 2′-[1-(2-pyridinyl)ethylidene]oxalohydrazide molecules was synthesized from bis(acetyl-acetonato)copper(II) and 2′-[1-(2-pyridinyl)ethylidene]oxamohydrazide. The x-ray analysis confirmed the tridentate coordination in the monoanionic form. The stable tetrahedral Cu(II) complex with one ligand molecule coordinated as a tridentate in the dianionic form was prepared by direct synthesis of $Cu(NO_3)_2 \cdot 3H_2O$ and Hapsox [20]. Complexes of bis[1-(pyridin-2-yl)ethylidene]oxalohydrazide have been prepared with Cr^{+3}, Mn^{+2}, Fe^{+3}, Co^{+2}, Ni^{+2}, Cu^{+2}, Cd^{+2}, VO^{+2} and Ag^{+} and characterized. The IR spectra showed the bidentate, tridentate or tetradentate behavior [21].

The present work aims to extend our work to prepare and characterize new complexes of bis[1-(pyridin-2-yl)ethylidene]malonohydrazide).

2. EXPERIMENTAL

2.1. Materials and Instrumentation

All chemicals were purchased from Aldrich or Fluka and used without further purification. The metal salts used are: $Co(OAc)_2.4H_2O$, $Ni(OAc)_2.4H_2O$, $Cu(OAc)_2.H_2O$, $Cd(OAc)_2.2H_2O$, $FeCl_3.6H_2O$, $MnCl_2.4H_2O$, $CrCl_3.3H_2O$, $AgNO_3$ and $VOSO_4$. Elemental analyses (C, H and some N) were performed with a Perkin-Elmer 2400 series II analyzer. The metal ions were determined complexometrically using EDTA titrations. Molar conductance values of 10^{-3} mol L^{-1} of the complexes, in DMSO, were measured using a Tacussel conductivity bridge model CD6NG. IR spectra (4000 - 400 cm^{-1}) were recorded on a Mattson 5000 FTIR spectrophotometer. Electronic spectra were recorded on a Unicam UV-Vis spectrophotometer UV_2. ^1H NMR measurements in d6-DMSO at room temperature were carried out on a Varian Gemini WM-200 MHz spectrometer at the Microanalytical Unit, Cairo University. ESR spectra for the Cu(II) complexes were obtained on a Bruker EMX spectrometer working in the X-band (9.78 GHz) with 100 kHz modulation frequency. The microwave power and modulation amplitudes were set at 1 mW and 4 Gauss, respectively. The low field signal was obtained after 4 scans with 10 fold increase in the receiver again. A powder spectrum was obtained in a 2mm quartz capillary at room temperature**.** Magnetic susceptibilities were measured with a Sherwood scientific magnetic susceptibility balance at 298 K. Thermogravimetric measurements (TGA, DTA) were recorded at 20–1000 ^oC on a DTG-50 Shimadzu thermogravimetric analyzer at a heating rate of 10 ^oC/min and nitrogen flow rate of 20 ml/min.

ISSN 2291-6458 (Print), ISSN 2291-6466 (Online)
Year 2013 | Volume 1 | Issue 4 | Page 277-291

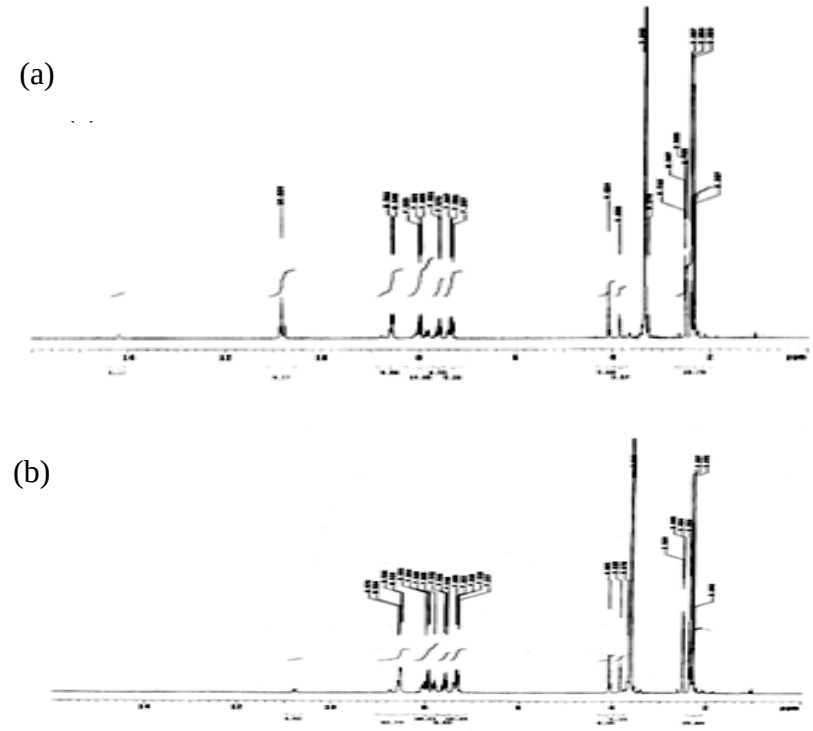

Figure 1. ^{1}H NMR spectra of H_2L (a) in DMSO (b) in D_2O

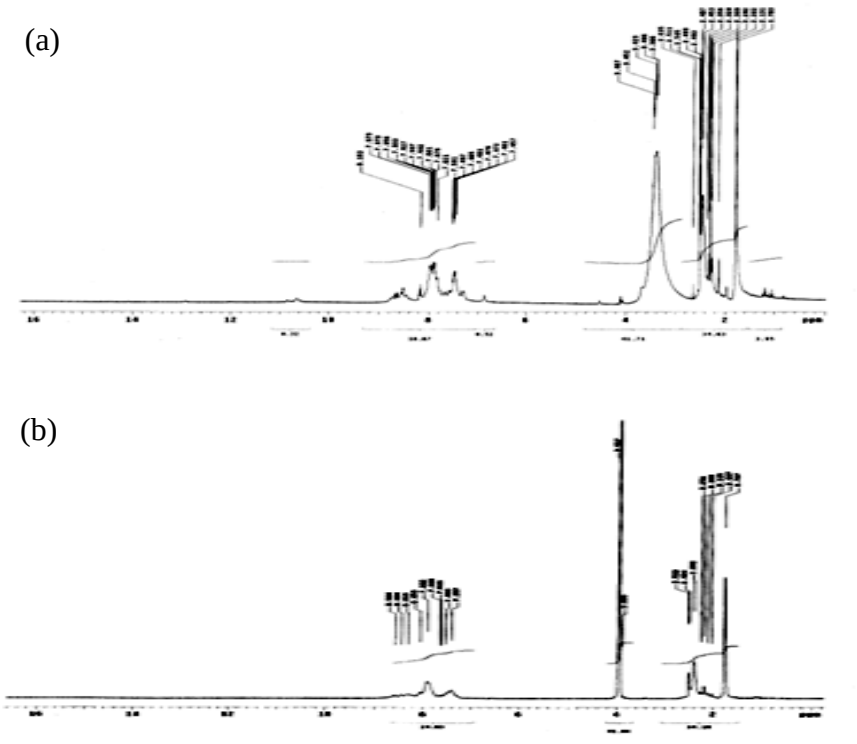

Figure 2. ^{1}H NMR spectra of $[Cd(H_2L)(OAc)_2].2H_2O$ (a) in DMSO (b) in D_2O

ISSN 2291-6458 (Print), ISSN 2291-6466 (Online)
Year 2013 | Volume 1 | Issue 4 | Page 277-291

Table 1. Analytical and physical data of H_2L and its metal complexes

Compound, Empirical formula	Yield (%)	Color	M.P. °C	% Found (Calcd.)					Λ^o_m in DMSO
				C	H	M	Cl	N	
H_2L $C_{17}H_{18}N_6O_2$	95	buff	252-3			-	-	-	-
$[Cu(H_2L)(OAc)_2].H_2O$ $CuC_{21}H_{26}N_6O_7$	75	Green	>300	46.90 (46.86)	5.28 (4.87)	11.61 (11.81)	-		1.36
$[Co_2(L)(OAc)_2(H_2O)_2].H_2O$ $Co_2C_{21}H_{30}N_6O_9$	80	Deep olive green	>300	44.42 (44.29)	5.17 (5.31)	10.31 (10.34)	-		0.37
$[Ni(H_2L)(OAc)_2(H_2O)].H_2O$ $NiC_{21}H_{28}N_6O_8$	75	Brownish yellow	>300	45.89 (45.76)	5.10 (5.12)	10.08 (10.65)	-		56.28*
$[Fe(HL)Cl_2(H_2O)]$ $FeC_{17}H_{17}N_6O_{23}Cl_2$	88	Brown	Chare at 187-200	42.75 (42.35)	4.26 (3.97)	11.21 (11.58)	14.52 (14.70)		39.15
$[Cr(H_2L)Cl_3].2H_2O$ $CrC_{17}H_{22}N_6O_4\ Cl_3$	85	Green	Chare at 285	38.92 (38.33)	4.79 (4.16)	10.12 (9.76)	20.27 (19.96)	15.77 (15.44)	27.63
$[Mn(H_2L)Cl_2(H_2O)].2H_2O$ $MnC_{17}H_{24}N_6O_5Cl_2$	80	Yellowish orange	Chare at 230-240	39.64 (39.39)	4.71 (4.66)	10.50 (11.60)	14.00 (13.68)		42.90
$[(VO)_2(L)(OH)_2].2H_2O$ $(VO)_2C_{17}H_{22}N_6O_5$	85	Pale brown	>300	38.00 (37.79)	4.20 (4.10)	- -	-	15.55 (15.64)	12.66
$[Cd(H_2L)(OAc)_2].2H_2O$ $CdC_{21}H28N_6O8$	75	Yellow	Chare at 250	41.10 (41.69)	4.25 (4.66)	19.00 (18.58)	-		3.04
$[Ag(H_2L)NO_3].EtOH$ $AgC_{19}H_{24}N_7O_6$	80	Gray	265-270	40.43 (40.01)	5.50 (4.24)	18.60 (18.91)	-	17.19 (17.34)	-

*conductance value in H_2O, $Ohm^{-1}cm^2mol^{-1}$

2.2. Synthesis of the ligand

$N^{1'}$,$N^{2'}$-bis(1-(pyridin-2-yl)ethylidene)malonohydrazide is prepared similar to $N^{1'}$,$N^{2'}$-bis[1-(pyridin-2-yl)ethylidene]oxalohydrazide [21] by heating mixture of malonic acid dihydrazide (7.80 g, 0.06 mol) and 2-acetylpyridine (13.44 ml (0.12 mol) in 30 ml ethanol. The mixture was heated under reflux for 3 h, evaporated and after cooling, white crystals were formed. The precipitate was filtered off, recrystallized from ethanol and dried. The purity was checked by TLC. The melting point is 252-3 ºC.

2.3. Synthesis of the complexes

A hot ethanol or aqueous-ethanol solution of metal acetate [Co(II), Ni(II), Cd(II)] or $CrCl_3$, $MnCl_2$, $FeCl_3$, $AgNO_3$ (1.0 mmol) and $VOSO_4$ (2.0 mmol), was added to a hot ethanol solution of H_2L (0.324 g, 1.0 mmol). The resulting mixture was heated under reflux for 2-3 h. The formed precipitates were filtered off, washed with ethanol followed by diethyl ether and dried. $[Co_2(L)(OAc)_2(H_2O)_2].H_2O$ and $[(VO)_2(L)(OH)_2].H_2O$ were isolated by mixing of $Co(OAc)_2$ or $VOSO_4$ and H_2L solutions in molar ratio 2:1 (M:L). The physical and analytical data of the isolated complexes are listed in Table 1. The complexes have high melting points, insoluble in common organic solvents and soluble in DMSO and DMF except for the Co(II) and Ni(II) complexes which are partially soluble. Molar conductance measurement indicates non-electrolytic nature of the complexes [22].

ISSN 2291-6458 (Print), ISSN 2291-6466 (Online)
Year 2013 | Volume 1 | Issue 4 | Page 277-291

Table 2. Important IR spectral bands of H_2L^2 and its metal complexes

Compound	ν(NH)	ν(C=O)	ν(C=N)$_{azo}$	ν(C=N)$_{py}$	ν(C=N*)	ν(C-O)	ν(N-N)	ν(M-O)	ν(M-N)	ν(O-H)*
H_2L	3191	1674	1629	1581	-	-	1046	-	-	-
$[Cu(H_2L)(OAc)_2].H_2O$	3077	1678	1595	1566	-	-	1022	566	460	3413
$[Co_2(L)(OAc)_2(H_2O)_2].H_2O$	3085	1706	1600	1565	-	-	1076	566	466	3421
$[Ni(H_2L)(OAc)_2(H_2O)].H_2O$	2929 3100	1636	1616	1566	-	-	1074	571	459	3406
$[Fe(HL)Cl_2(H_2O)]$	3099	1686	1620	1553	1600	1255	1020	580	434	3390
$[Cr(H_2L)Cl_3].2H_2O$	3073	1673	1598	1556	-	-	1027	580	433	3367
$[Mn(H_2L)Cl_2(H_2O)].2H_2O$	3177	1671	1596	1566	-	-	1051	567	479	3381
$[(VO)_2(L)(OH)_2].2H_2O$	3108	-	-	1558	1604	1259	1033	555	479	3419
$[Cd(H_2L)(OAc)_2].2H_2O$	3006	1664	1562	1562	-	-	1033	566	447	3403
$[Ag(H_2L)NO_3].EtOH$	3097	1685	1614	1584	-	-	1036	511	426	

2.4. Superoxide dismutase (SOD) scavenging activity

SOD activity of the investigated compounds was assayed by using phenazen methosulfate (PMS) [23] to photogenerate a reproducible and constant flux of superoxide anion radicals at pH = 8.3 (phosphate buffer). Reduction of nitroblue tetrazolium (NBT) to blue formazan was used as an indicator of O_2^- production and followed spectrophotometrically at 560 nm. The addition of PMS (9.3 x 10^{-4}M) to an aqueous solution of NBT (3.0x 10^5 M), NADH (nicotineamideadinine dinucloted, 4.7x 10^{-4}M, and phosphate buffer (final volume of 2 ml) caused a OD(Δ_{560})/min change. The reaction in blank sample and in presence of the compounds under study was measured for 3 min. The inhibition percent was calculated using the equation:

$$\% \text{ Inhibition} = \Delta B - \Delta S / \Delta B \times 100$$

Where $\Delta B = A_{3min} - A_{zero}/3$; Δ is the change in absorbance from 0 to 3 minutes for the standard i.e. ascorbic acid (B) and the sample (S), respectively.

2.5. Molecular modeling

An attempt to gain a better insight on the molecular structure of the ligand and its complexes, geometric optimization and conformational analysis has been performed by the use of MM+ force field as implemented in hyperchem 8.0 [24]. The geometry with minimum energy obtained from MM+ was optimized with the Semi-Empirical Parametrization Model 3 (PM3) using the Polak-Ribiere algorithm in RHF-SCF, set to terminate at an RMS gradient of 0.0419 kJ $Å^{-1}$ mol^{-1} and the convergence limit was fixed to 4.187×10^{-8} kJ mol^{-1}.

3. RESULTS AND DISCUSSION

The data of elemental analysis together with some physical properties of the complexes are summarized in Table 1.

ISSN 2291-6458 (Print), ISSN 2291-6466 (Online)
Year 2013 | Volume 1 | Issue 4 | Page 277-291

3.1 IR and ^{1}H NMR spectra

The most characteristic IR bands of H_2L and its complexes with their assignments are recorded in Table 2. The IR spectrum of H_2L exhibits bands at 3191, 1629, 1674 1581, 1046 and 993 cm^{-1} assigned to ν(NH), $\nu(C=N)_{azo}$, ν(C=O), $\nu(C=N)_{py}$, ν(N–N) and pyridine ring [25-29]. Its ^{1}H NMR spectrum, in d_6-DMSO solution (Fig. 1) shows signals at δ = 14.20 (s, 1H) and 10.66 (t, 1H) ppm assignable to the protons of OH (the enolized form of CONH) and NH [28]. The first signal disappeared upon adding D_2O while the second becomes weak. The signal attributed to the methyl protons (6H) appeared at 2.32 ppm while those of pyridine rings (8H) are observed as multiple peaks at 7.33 (t, 2H, H–C_5; H–C_{18}, 3J = 5.0 Hz, 3J = 1.5 Hz), 7.57 (dt, 2H, H–C_4; H–C_{19}, 3J = 7.5 Hz, 3J = 1.5 Hz), 7.95 (dt, 2H, H–C_3; H–C_{20}, 3J = 7.5 Hz),8.56 (dt, 2H, H–C_6; H–C_{17}, 3J = 5.0 Hz), 10.82 (bs, 2H, H–N_9; H–N_{14}). The numbering of the atoms in H_2L is shown in Structure 1.

A comparison of the IR spectra of H_2L and its metal complexes depicts different chelation modes. H_2L behaves as a neutral NNO in $[Cr(H_2L)Cl_3].2H_2O$, $[Mn(H_2L)(H_2O)Cl_2].2H_2O$ and $[Cd(H_2L)(OAc)_2].2H_2O$ coordinating *via* $C=N_{azo}$, $C=N_{py}$ and C=O as indicated by the shift of their bands to lower wavenumbers. The appearance of new bands at 566-580 and 433-479 cm^{-1} due to ν(M-O) and ν(M-N)[30] supporting their coordination. The broad bands at 1521and 1371 cm^{-1} assigned to ν_{as}(OAc) and ν_s(OAc) with difference of 150 cm^{-1}, in the spectrum of Cd(II) complex, confirm the monodentate nature of the acetate group [31]. The ^{1}HNMR spectrum (Fig. 2) of Cd complex, in d_6DMSO, shows no signal assignable to the OH proton excluding the possibility of enolization of the carbonyl group. The signal due to NH protons undergoes weakness as a result of coordination of C=N.

H_2L also behaves as a monobasic NNOO in $[Cu(H_2L)(OAc)_2].H_2O$ *via* $C=N_{azo}$, $C=N_{py}$, C=O and C-OH by removing the amide proton (HN-C=O → N=C–O–). The shift of ν(C=O) to lower wavenumber and the disappearance of ν(NH) confirm that one of the carbonyl groups participates in coordination and indicated by the appearance of new bands at 1595, 1251, 566 and 460 cm^{-1} assigned to ν(C=N*), ν(C-O), ν(M-O) and ν(M-N) [30]**.** The broad bands at 1566 and 1377 cm^{-1} (Δν=189 cm^{-1}**)** confirm the monodentate nature of the acetate group [31].

In $[Fe(HL)(H_2O)Cl_2]$ and $[Ni(H_2L)(OAc)_2(H_2O)].H_2O$, H_2L binds as a monobasic NNO *via* enolized C-O, $C=N_{py}$ and $C=N_{azo}$ groups by: i) the weakness of the band due to ν(C=O) suggesting that one carbonyl group participates in coordination by removing the amide proton while the second one remains uncoordinated. This is confirmed by the appearance of new bands at 1255 & 1257 and 1600 & 1597 cm^{-1} attributable to ν(C-O) and ν(N^*=C-C=N*). ii) The shift of $C=N_{azo}$ to higher wavenumber. iii) The bands at 1507 and 1314 cm^{-1} with difference of 193 cm^{-1} in Ni(II) spectrum is characteristic for the monodentate acetate nature [31].

Another mode of chelation is depicted in $[(VO)_2(L)(OH)_2].2H_2O$ and $[Co_2(L)(OAc)_2(H_2O)_2].H_2O$ (Structure 2), where the ligand coordinates as N_4O_2 *via* two $C=N_{azo}$, two C-O and two $C=N_{py}$ supporting by: i) the disappearance of ν(C=O) with the appearance of 1259 (1257) cm^{-1} band due to ν(C-O); ii) the shift of $C=N_{azo}$ to lower wavenumber; iii) the new band at 1604 (1600) cm^{-1} is attributed to ν(N^*=C); iv) the participation of $C=N_{py}$ is confirmed by the shift of its band to lower wavenumber; v) the band at 980 cm^{-1} is characteristic for ν(V=O) [31]; vi) the new band at 508 cm^{-1} is due to ν(V-O) [32]. The acetate in $[Co_2(L)(OAc)_2(H_2O)_2].H_2O$ acts as a bidentate ligand by the appearance of 1502 and 1411 cm^{-1} with Δν = 91 cm^{-1} [30].

ISSN 2291-6458 (Print), ISSN 2291-6466 (Online)
Year 2013 | Volume 1 | Issue 4 | Page 277-291

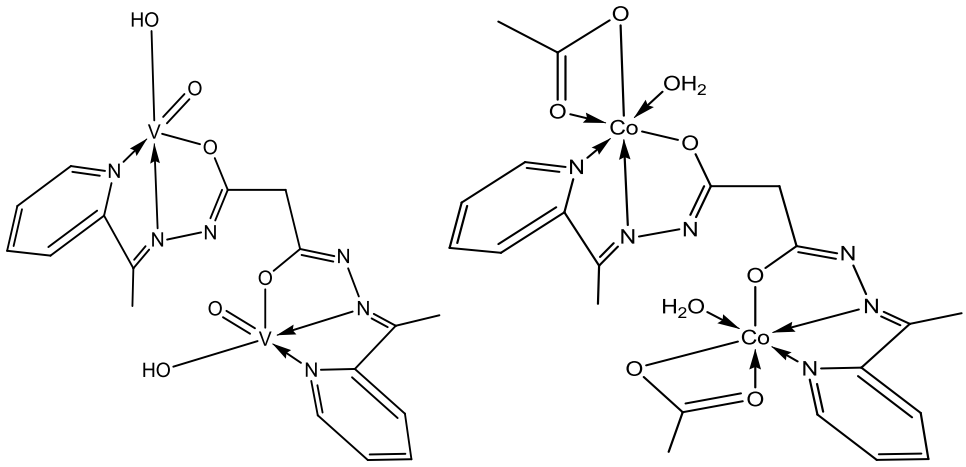

Structure 2. Proposed structures for $[(VO)_2(L)(OH)_2].2H_2O$ and $[Co_2(L)(OAc)_2(H_2O)_2].H_2O$

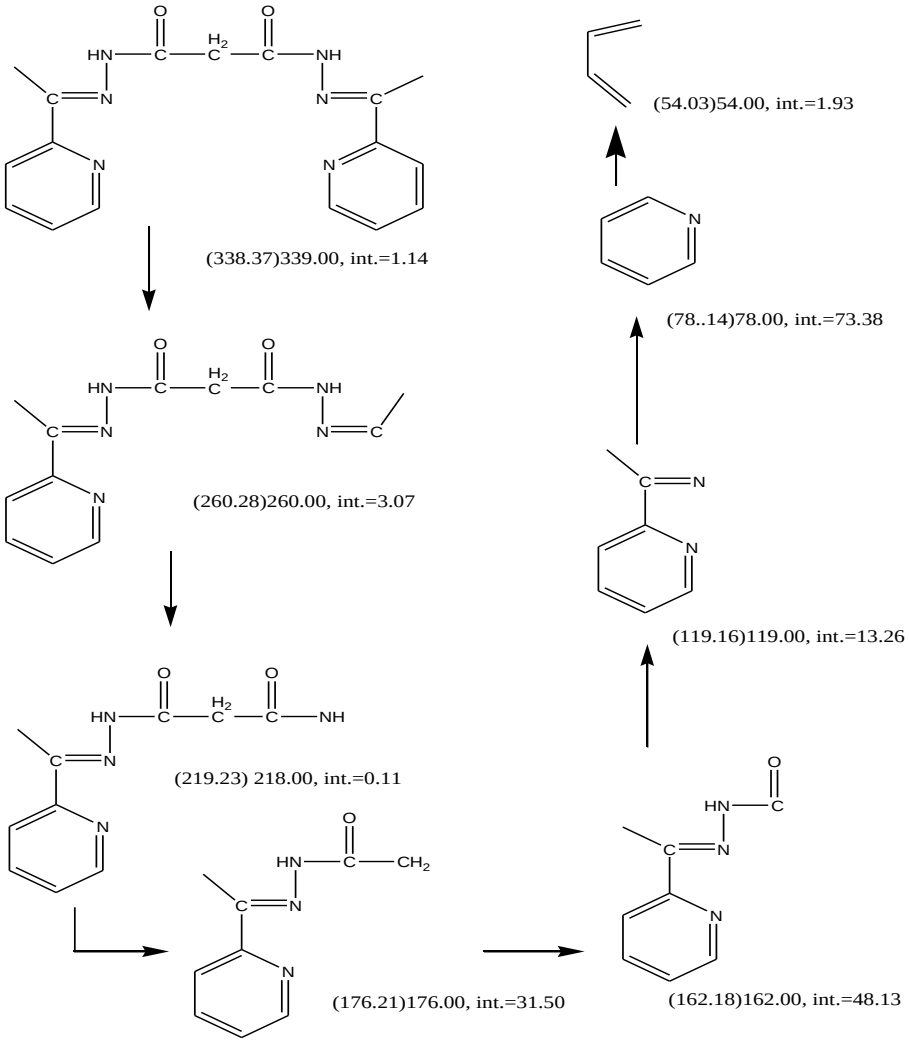

Scheme 1. Fragmentation pattern of H_2L based on mass spectra

ISSN 2291-6458 (Print), ISSN 2291-6466 (Online)
Year 2013 | Volume 1 | Issue 4 | Page 277-291

Finally, H_2L acts as a neutral bidentate in $[Ag(H_2L)NO_3].EtOH$ coordinating *via* $C=N_{azo}$ and C=O. The spectrum exhibits bands at 1468 and 1329 cm^{-1} assigned to $\nu_5(NO_3)$ and $\nu_1(NO_3)$ with difference of 139 cm^{-1} supporting its unidentate nature [33]. The ^{1}HNMR spectrum (Fig. 1S) showed two doublets at 11.33 and 10.86 ppm. The coordinated water shows broad bands at 3367-3421, 811-898, and 555-580 cm^{-1} referring to $\nu(H_2O)$, $\rho_r(H_2O)$ and $\rho_w(H_2O)$. However, the hydrated water exhibits a broad band centered at 3500 cm^{-1}. To verify between them, TGA was recorded.

3.2 Mass spectra

The mass spectrum of H_2L (Scheme 1) shows the molecular ion peak at m/e = 339 in accordance with its molecular mass. The peaks at 260 (Calcd. 260.28), 218 (Calcd. 219.23), 176 (Calcd. 176.21), 162 (Calcd. 162.18), 119 (Calcd. 119.16), 78 (Calcd. 78.14) and 54.00 (Calcd.54.03) are corresponding to the removal of pyridine, C_2H_3N, CHNO, CH_2, CHNO and finally C_4H_6 as a residue.

3.3 Electronic spectra and magnetic moments

The UV spectrum of H_2L and the electronic spectra of its complexes were recorded in DMF and Nujol. The characteristic bands, magnetic moments and ligand field parameters are given in supplementary Table 1S. The spectrum of the ligand shows absorption band at 33560 cm^{-1} assigned to the $\pi \rightarrow \pi^*$ transition and two strong absorption bands at 31445 and 27030 cm^{-1} attributed to the $n \rightarrow \pi^*$ transition of the carbonyl and azomethine groups. Large change is observed on the spectra of its complexes with new $n \rightarrow \pi^*$ bands at 41670 - 33330 cm^{-1} and 26315 - 27470 cm^{-1}.

The electronic spectrum of $[Cu(H_2L)(OAc)_2(H_2O)].H_2O$ shows bands at 14165 cm^{-1} in DMF (14580 and 17670 cm^{-1} in Nujol) assigned to $^2B_{1g} \longrightarrow {}^2B_{2g}$ and $^2B_{1g} \longrightarrow {}^2E_g$ in a tetragonal octahedral structure. The appearance of a higher energy band at (25510 -26740 cm^{-1} in Nujol) may be due to L→MCT. The magnetic moment value (1.44 BM) is subnormal due to copper-copper interaction.

The electronic spectrum of $[Co_2(L)(OAc)_2(H_2O)_2].H_2O$ exhibits two bands at 21010 and 16130 cm^{-1} in Nujol assigned to $^4T_{1g} \longrightarrow {}^4T_{1g}$ (P) and $^4T_{1g} \longrightarrow {}^4A_{2g}$ in a high-spin octahedral complexes [34]. The magnetic moment value (3.41 BM/Co atom) confirms the presence of three unpaired electrons with no orbital contribution. The calculated values of the ligand field parameters (Dq, B and β) are 976.66 cm^{-1}, 745.68 cm^{-1} and 0.77, respectively.

The electronic spectrum of $[Ni(H_2L)(OAc)_2(H_2O)].H_2O$ exhibits two bands at 12320 and 22830 cm^{-1} in Nujol assignable to $^3A_{2g} \longrightarrow {}^3T_{1g}$ and $^3A_{2g} \longrightarrow {}^3T_{1g}$(P) in octahedral structure [25]. The calculated values of Dq, B and β are 739.01cm^{-1}, 869.42 cm^{-1} and 0.83 as well as the magnetic moment value (3.64 BM) are consistent with Ni(II) octahedral geometry.

The electronic spectrum of $[Fe(HL)Cl_2(H_2O)].H_2O$ shows three bands at 16290, 19685 and 25770 cm^{-1}, in Nujol, attributed to $^6A_{1g} \longrightarrow {}^4T_{1g}$(G), $^6A_{1g} \longrightarrow {}^4T_{2g}$ (G) and $^6A_{1g} \longrightarrow {}^4E_g$(G) in an octahedral configuration [35]. The magnetic moment value (6.77 BM) is in good evidence with the proposed geometry.

The electronic spectrum of $[Cr(H_2L)Cl_3].2H_2O$ shows two bands at 18660 and 25510 cm^{-1} assignable to $^4A_{2g} \longrightarrow {}^4T_{2g}(\nu_1)$ and $^4A_{2g} \longrightarrow {}^4T_{1g}(\nu_2)$ in an octahedral geometry [36]. The $^4A_{2g} \longrightarrow {}^4T_{1g}(P)(\nu_3)$ band is expected to be at 31450 cm^{-1} generally covered by the broad charge transfer band. The B value (668.04 cm^{-1}) is calculated by the equation [37]:

$$B = (2\nu_1^2 - 3\nu_1\nu_2 + \nu_2^2) / (15\nu_2 - 27\nu_1)$$

From this equation, the values of Dq and β are 1865.70 cm^{-1} and 0.73. The Dq, B, β and ν_2/ν_1 values as well as the magnetic moment (4.82 BM) confirm an octahedral structure. The high β value indicates a less covalency for the Cr-H_2L bonds.

ISSN 2291-6458 (Print), ISSN 2291-6466 (Online)
Year 2013 | Volume 1 | Issue 4 | Page 277-291

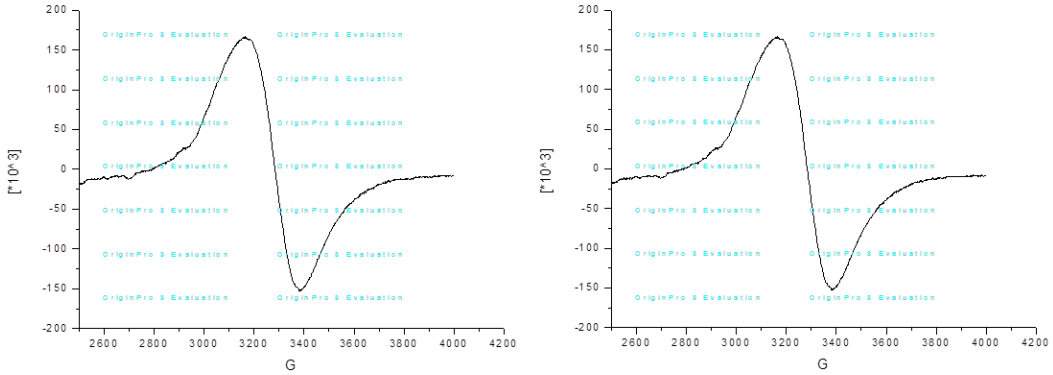

Figure 3. ESR spectrum of $[Cu(H_2L)(OAc)_2].H_2O$ (left) and $[(VO)_2(L)(OH)_2].2H_2O$ (right)

The electronic spectrum of $[(VO)_2(L)(OH)_2].2H_2O$ exhibits a band at 12790 cm^{-1} assignable to $^2B_2 \rightarrow {}^2E(\nu_1)$ in a square - pyramid configuration [38]. The existence of the band at 980 cm^{-1} in its IR spectrum and the pale brown color are good evidence for the proposed structure. The magnetic moment (1.59 BM/V atom) is less than those reported for the spin only moment due to the presence of one electron and may consistent with those reported for binuclear complexes.

$[Mn(H_2L)Cl_2(H_2O)].2H_2O$ exhibits two bands at17610 and 24270 cm^{-1} in Nujol due to $^6A_{1g} \longrightarrow {}^4T_{1g}(G)$ and $^6A_{1g} \longrightarrow {}^4T_{2g}(G)$ in an octahedral geometry [39]. The value of its magnetic moment (7.47 BM) is consistent with those reported for high spin d^5 system.

In $[Cd(H_2L)(OAc)_2].2H_2O$, the $\pi \rightarrow \pi^*$, $n \rightarrow \pi^*$ and LMCT transition bands are located at 34015, 27935 and 24270 cm^{-1}. $[Ag(H_2L)NO_3].H_2O$ exhibits bands at 36495 and 31645 cm^{-1} attributing to intraligand and CT transitions. The band at 27030 cm^{-1} is an evidence for the participation of C=N lone pair electrons [40].

3.4 ESR spectra

The room temperature solid state ESR spectrum of $[Cu(H_2L)(OAc)_2].H_2O$ (Fig. 3 left) shows an intense and broad signal without hyperfine splitting (g_{iso}=2.13). The higher g value, when compared to that of free electron (g= 2.0023) revealing an appreciable covalency of the metal ligand bonding with d_{x2-y2} as ground-state [41] characteristic of a square-planar, square- pyramidal or octahedral stereochemistry [42]. In order to quantify the degree of distortion of the Cu(II) complex, $f(\alpha)=g_{\|}/A_{\|}$ is selected. Values of $f(\alpha)$=110-120 are typical for planar complexes, while 130-150 is characteristic for slight to moderate distortion and 180-250 cm^{-1} indicate considerable distortion [31]. The calculated value for the present complex (161 cm^{-1}) lies within the range expected for octahedral or square - pyramidal complex [43].

The ESR spectrum of powdered $[(VO)_2(L)(OH)_2].2H_2O$ (Fig. 3 right) gave a single broad line centered at g=1.97, without resolved hyperfine structure. In particular, the hyperfine coupling with ^{51}V (I=7/2) nucleus is not observed. The absence of vanadium hyperfine coupling is attributed to the simultaneous flipping of neighboring electron spins [32] or due to strong exchange interactions of dimeric or polymeric structure. Generally, the mononuclear VO^{2+} ion (S=1/2, I=7/2) has a characteristic octet ESR spectrum showing the hyperfine coupling to the ^{51}V nuclear magnetic moment. Upon the existence of two VO^{2+} ions, the two electron spins may combine to a nonmagnetic spin singlet (S=0) or a paramagnetic triplet (S=1); only the latter is ESR detectable. The super exchange interaction between the two vanadyl ions lead to a configuration in which the two electron spins have an antiferromagnetic character, i.e. the

ISSN 2291-6458 (Print), ISSN 2291-6466 (Online)
Year 2013 | Volume 1 | Issue 4 | Page 277-291

Table 3. Some energy of H_2L and its complexes calculated by PM3 method

Compound	Total Energy kcal/mol	Binding Energy kcal/mol	Electronic Energy kcal/mol	Heat of Formation kcal/mol	Dipole Moment D	HOMO ev	LUMO Ev
H_2L	-88775	-4589	-653480	50	2.33	-9.41	-0.42
$[Cu(H_2L).(OAc)_2].H_2O$	-155820	-5968	-1396043	-65	2.11	-7.93	-1.27
$[Co_2(L)(OAc)_2(H_2O)_2].H_2O$	-154825	-6672	-1474285	-531	5.06	-4.61	-0.55
$[Ni(H_2L)(OAc)_2(H_2O)].H_2O$	-160440	-6421	-1424312	-280	3.95	-7.73	-1.36
$[Cr(H_2L)Cl_3].2H_2O$	-116652	-5024	-994141	-202	9.94	-3.96	-2.49
$[Mn(H_2L)Cl_2(H_2O)].2H_2O$	-119975	-5087	-970102	-158	3.10	-4.28	-0.51
$[Cd(HL)(OAc)_2].2H_2O$	-116855	-5496	-967985	-49	3.89	-3.93	-0.23

Table 4. Effect of ligand and its metal complexes on superoxide radicals generated by PMS/NADH-NBT system

Compound	Δ through 3 min	% inhibition
L-ascorbic acid	0.0033	87.86
H_2L	0.0870	4.80
$[Cu(H_2L)(OAc)_2].H_2O$	0.0030	96.00
$[Co(H_2L)(OAc)_2(H_2O)].2H_2O$	0.0040	95.00
$[Ni(H_2L)(OAc)_2(H_2O)].H_2O$	0.0410	51.00
$[Mn(H_2L)Cl_2(H_2O)].2H_2O$	0.0240	71.00
$[Fe(HL)(H_2O)Cl_2]$	0.0020	98.00
$[Ag(H_2L)NO_3].H_2O$	0.0490	41.00
$[(VO)_2(L)(OH)_2].2H_2O$	0.0570	31.20
$[Cd(H_2L)(OAc)_2].2H_2O$	0.0440	47.00

singlet state is energetically favored. Therefore, the ESR spectrum of strongly coupled pairs has the form of a single broad line with non-homogeneous broadening. The data agree well with the subnormal magnetic moment value (μ_{eff} =1.59 BM) and confirming a dimeric or a polymeric structure. Also, the decrease of the g value than that of the free-electron value (2.0023) is a measure of the ligand field strength.

3.5 Thermal studies

The stages of decomposition, temperature range, decomposition product as well as the weight loss

ISSN 2291-6458 (Print), ISSN 2291-6466 (Online)
Year 2013 | Volume 1 | Issue 4 | Page 277-291

percentage of some metal complexes are given in supplementary Table S2.

The thermogram of $[Cu(H_2L)(OAc)_2].H_2O$ displays a step at 37-138 ^oC with weight loss of 3.84 (Calcd. 3.35 %) corresponding to the loss of water. The second step with weight loss of 36.58 (Calcd. 36.46%) at 139-399 ^oC is attributed to the elimination of $2OAc+C_5H_4N$. The third step at 400-602 ^oC with weight loss of 45.00 (Calcd. 45.42 %) is referring to the removal of $C_5H_4N+CONH+CNH+CH_2+2CNCH_3$. The residual part is CuO (Found 14.58; Calcd. 14.77 %).

The TGA of $[Co_2(L)(OAc)_2(H_2O)_2].H_2O$ shows five steps. The first step at 39-88 ^oC with weight loss of 2.68 (Calcd. 2.87%) is corresponding to the loss the lattice water. The second step with weight loss of 15.02 (Calcd. 15.17%) at 88-201 ^oC is attributed to the elimination of $2H_2O+OAc$. The third step at 297-479 ^oC with weight loss of 28.21 (Calcd. 28.44 %) is referring to the removal of $C_5H_4N+OAc+CNCH_3$. The fourth step at 479-602 ^oC with weight loss of 19.33 (Calcd. 19.02%) is referring to the removal of $C_5H_4N+CNCH_3$. The fifth step at 602-748 ^oC with weight loss of 10.55 (Calcd. 10.75%) is referring to the removal of $2CN+CH_2$.The residue is 2CoO (Found 24.01, Calcd. 23.93 %).

The thermogram of $[Ni(H_2L)(OAc)_2(H_2O)].H_2O$ displays the first at 39-209 ^oC with weight loss of 3.70 (Calcd. 3.27 %) corresponding to the loss of hydrated H_2O. The second with weight loss of 38.49 (Calcd. 38.86%) at 311-425 ^oC is due to the elimination of $C_5H_4N+H_2O+2OAc$. The third at 425-650 ^oC with weight loss of 44.83 (Calcd. 44.32 %) is referring to the removal of $2CNCH_3+CONH+CNH+-CH_2+C_5H_4N$. The residual part is NiO (Found 12.98; Calcd. 13.55 %).

The thermogram of $[(VO)_2(L^2)(OH)_2].2H_2O$ displays the first step at 38-150 ^oC (weight loss of 6.34; Calcd. 6.67 %) corresponding to the loss of two lattice water molecule. The second step (weight loss of 20.88; Calcd 20.75 %) at 257-371 ^oC is attributing to the elimination of C_5H_4N+2OH. The third step at 372-458 ^oC with weight loss of 22.56 (Calcd. 22.05 %) is referring to the removal of $CNCH_3+C_5H_4N$. The fourth step at 458-568 ^oC with weight loss of 19.30 (Calcd. 19.82 %) is referring to the removal of $CNCH_3+2CN+CH_2$. The residual part is $2VO_2$ with weight loss of 30.92 (Calcd. 30.70 %).

3.6 Thermodynamic and kinetic studies: *Coats-Redfern method*

The equation of Coats-Redfern [44] method is: $\ln[\frac{g(\alpha)}{T^2}] = \ln\left(\frac{AR}{\beta E}\right) - \frac{Ea}{RT}$

Where $g(\alpha) = 1- (1 - \alpha)^{1-n}/1-n$ for $n \neq 1$ and $g(\alpha) = - \ln(1 - \alpha)$ for n=1, R is the universal gas constant. The correlation coefficient, r, was computed using the least square method for different values of n (n=0.33, 0.5, 0.66 and n=1) by plotting $\ln[\frac{g(\alpha)}{T^2}]$ versus 1/T for the investigated metal complexes. The n-value which gave the best fit ($r \approx 1$) was chosen as the order parameter for the decomposition stage of interest. The slope of the straight line equal (E/R) and the intercept the pre- exponential factor, A can be determined.

3.7 Thermodynamic parameters

The kinetic parameters reveal the following: ΔS^* is negative for some decomposition steps indicating that the activated fragments are more ordered than the un-decomposed ones [45]. The positive sign of ΔH^* indicates that the decomposition stages are endothermic processes. The high values of Ea reveal the high stability of such chelate due to their covalent bond character. The positive sign of ΔG^* reveals that the free energy of the final residue is higher than that of the initial compound and hence all

ISSN 2291-6458 (Print), ISSN 2291-6466 (Online)
Year 2013 | Volume 1 | Issue 4 | Page 277-291

decomposition steps are nonspontaneous. Moreover, the values of ΔG* increase significantly for the subsequent decomposition steps of a given compound resulting from increasing TΔS*. This may be attributed to the structural rigidity of the remaining complex after the expulsion of one or more ligands.

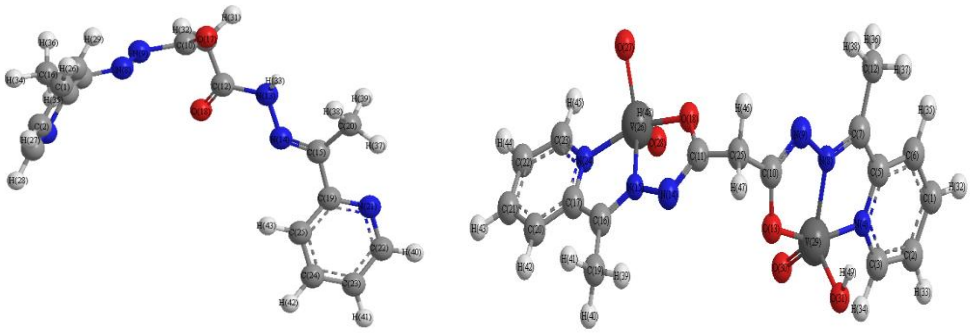

Structure 3. Molecular structure of H_2L, obtained from molecular modeling with MM^+ and PM3 methods
Molecular structure of $[(VO)_2(L)(OH)_2].2H_2O$, obtained with MM^+ and PM3 methods

3.8. Molecular modeling

Analysis of the molecular modeling data, one can conclude the following remarks: there is a large variation in N_{13}-N_{14} bond lengths on complexation. It becomes either short as in $[Cu(H_2L)(OAc)_2].H_2O$, $[Fe(HL)Cl_2(H_2O)]$ and $[Cd(H_2L)(OAc)_2].2H_2O$ or long as in $[Ag(H_2L)NO_3].EtOH$, $[Cr(H_2L)Cl_3].2H_2O$, $[Ni(H_2L)(OAc)_2(H_2O)].H_2O$, $[Co_2(L)(OAc)_2.(H_2O)_2].H_2O$ and $[Mn(H_2L)Cl_2(H_2O)].2H_2O$ as the coordination takes place *via* C=N and C-O. The bond lengths of N_1-C_6 become shorter in $[(VO)_2(L)(OH)_2].2H_2O$ (Structure 4) as the coordination takes place via N atoms of *N=C-C=N*- group that is formed on deprotonation of two C-OH groups. The C_{12}-O_{18} and C_{14}-N_{15} bond distances in all complexes become shorter due to the formation of strong M-O bond which makes the C-O bond weak except in $[Cr(H_2L)Cl_3].2H_2O$ which this bond is elongated referring to the formation of M-O bond which makes the C-O bond weak and forming a double bond character. The bond angles of the hydrazone moiety of H_2L are altered somewhat upon coordination; the largest change affects N_{14}-N_{13}- C_{15}, N_{13}-C_{12}-O_{18}, C_{10}-N_9-N_8 and N_9-N_8-C_7 angles which are reduced or increased on complex formation as a consequence of bonding. The N_{14}-N_{13}- C_{15} angle changes from 122.3° to (126.1°-121.9°) in all complexes due to the formation of the N_8-M-O_{11} chelate ring. The bond angles in complexes namely, $[Cr(H_2L)Cl_3].2H_2O$, $[Mn(H_2L)Cl_2.(H_2O)].2H_2O$, $[Fe(HL)Cl_2.H_2O]$ and $[Co_2(L)(OAc)_2(H_2O)_2].H_2O$ are quite near to a octahedral geometry. The lower HOMO values show that molecules donating electron ability is the weaker. On contrary, the higher HOMO energy implies that the molecule is a good electron donor. LUMO energy presents the ability of a molecule receiving electron (Table 3). The bond angles within the hydrazone backbone do not change significantly but the angles around the metal undergo appreciable variations upon changing the metal center.

3.9 Superoxide dismutase (SOD) scavenging activity

A glance at Table 4 indicated that there is an apparent variation in the overall scavenging ability among the ligand and its metal complexes. Fe(III), Cu(II) and Co(II) complexes exhibit a potent inhibition activity comparable to ascorbic acid. Mn(II), Cd(II) and Ni(II) complexes display scavenging activities greater than 50% of the superoxide radical. The Ag^+ and VO^{2+} complexes exhibit scavenging activity lower than 50%. On the other hand, the ligand exhibits no activity. Cu(II) complex revealed the highest scavenging activity

ISSN 2291-6458 (Print), ISSN 2291-6466 (Online)
Year 2013 | Volume 1 | Issue 4 | Page 277-291

of superoxide radical in this system. It is known that superoxide is a major factor in radiation damage, inflammation and tumor promotion. Fortunately, the present study has evolved a defense system against the toxicity of $O_2^{\bullet-}$ by the Cu(II) complex.

4. CONCLUSIONS

Transition metal complexes of N^1, N^3-bis(1-(pyridin-2-yl)ethylidene)malono-hydrazide (H_2L) have the formulae: $[Cu(H_2L)(OAc)_2].H_2O$; $[Co_2(L)(OAc)_2.(H_2O)_2].H_2O$; $[Ni(H_2L)(OAc)_2.H_2O].H_2O$; $[Ag(H_2L)NO_3].EtOH$; $[Cd(H_2L)(OAc)_2]$-$.2H_2O$; $[(VO)_2(L)(OH)_2].H_2O$; $[Mn(H_2L)(H_2O)Cl_2].2H_2O$; $[Cr(H_2L)Cl_3].2H_2O$ and $[Fe(HL)(H_2O)Cl_2]$. Different modes of chelation have been suggested for the ligand: neutral (bidentate or tridentate); monobasic (tridentate or tetradentate) and binegative hexadentate and supported by ^{1}HNMR for the diamagnetic complexes. All complexes have octahedral structure except for VO^{2+} complex which has a square-pyramid and intense color (green to brown). A variation in the overall scavenging ability was observed among the ligand and its metal complexes.

SUPPORTING INFORMATION

Figure 1S, and Table 1S and 2S are included in the supporting information. This document is available at http://canchemtrans.ca/uploads/files/Supporting_Information_0041.pdf

REFERENCES AND NOTES

[1] Dilworth, J. R. The coordination chemistry of substituted hydrazines. *Coord. Chem. Rev.* **1976**, *21*, 29-62.
[2] Siddappa, K.; Mane, S. B. Pharmacological activity of (E) 3-2-(1-(1-hydroxynaphalen-2-yl) methyleneamino) phenyl)-2-methylquinazoline-4 (3H)-one Schiff base and its transition metal complexes, *Int. J. Pharm. Pharmaceutical Sci.*, **2013,** *15*, 724-732.
[3] Aggarwal, R. C.; Tadav, B. N.; Prosad, T. Acyl hydrazine complexes of titanium and zirconium tetrachlorides. *J. Inorg. Nucl. Chem.* **1973,** *35*, 653-655.
[4] Jeewoth, T.; Bhowon, M. G.; Li, H.; Wah, K. Synthesis, characterization and antibacterial properties of Schiff bases and Schiff base metal complexes derived from 2,3-diamino- pyridine. *Transition Met. Chem.* **1999**, *24*, 445-448.
[5] Khalifa, M. E. Selective Flotation-Spectrophotometric Procedure for the Trace Analysis of Palladium (II) in Different Matrices. *Anal. Sci. Jpn.* **1999**, *15*, 433-438.
[6] Kabil, M. M.; Akl, M. A.; Khalifa, M. E. Selective Flotation-Spectrophotometric Procedure for the Trace Analysis of Palladium(II) in Different Matrices. *Anal. Sci. Jpn.* **1999**, *15*, 433-438.
[7] Ghazy, S. E.; Rakha, T. H.; El-Kady, E. H.; El-Asmy, A. A. Use of some hydrazine derivatives for the separation of mercury(II) from aqueous solutions by flotation technique. *Ind. J. Chem. Technology*, **2000**, *7*, 178-183.
[8] Katyal, M.; Dutt, Y. Analytical applications of hydrazones. Analytical applications of hydrazones. *Talanta* **1975**, *22*, 151-161.
[9] Katyal, M.; Dutt, Y. Analytical applications of hydrazones. Analytical applications of hydrazones. *Talanta* **1975**, *22*, 151-161.
[10] Bell, C. F.; Rose, D. R. Spectrophotometric determination of palladium with pyridsine 2-alkdehyde-2-pyridylhydrazone. *Talanta* **1965**, *12*, 696-700.
[11] Sears, J. K.; Darby, J. R. *The Technology of Plasticizers*, Wiley, New York, 1982.
[12] Massarani, E.; Nardi, D. Tajana, A.; Degen, L. Antibacterial nitrofuran derivatives. 2. 5-Nitro-2-furaldehyde aminoacethydrazones *J. Med. Chem.* 1971, *14*, 633-635.

ISSN 2291-6458 (Print), ISSN 2291-6466 (Online)
Year 2013 | Volume 1 | Issue 4 | Page 277-291

[13] Arapov, O. V.; Alferva, O. F.; Levocheskaya, E. I.; Krasilnikov, I. Radioprotective efficacy of acyl hydrazones. *Radiohiologiya*, **1987**, *27*, 843-846.

[14] Abram, S.l.; Maichle-Mossmer, C.; Abram, U. Synthesis and characterization of indium(III). *polyhedron* **1998**, *17*, 131-143.

[15] de Sousa, G. F.; Filgueiras, C.A.L.; Abras, A.; Al-Juaid, S.S.; Hitchcock, P.B.; Nixon, J. F. New heptacoordinated tin complexes of 2,6-diacetylpyridine-bis(thiosemicarbazone), H_2daptsc, and of 2,6-diacetylpyridine-bis(semi-carbazone), H_2dapsc. Crystal and molecular structures of [MeSnCl(Hdaptsc)]Cl·MeOH and [MeSnCl(H_2dapsc)]Cl_2·2H_2O. *Inorg. Chim. Acta* **1994**, *218*, 139.

[16] El-Metwally, N. M.; Al-Hazmi, G. A.; El-Asmy, A. A. Spectral, magnetic, electrical and thermal studies on malonyl bis(thiosemicarbazide) complexes. *Transition. Met. Chem.* **2006**, *31*, 673-677.

[17] Andjelkovic´, K.; Ivanovic´, I.; Niketic´, S.R.; Prelesnik, B.; Leovac, V. M. *Polyhedron* 1997, 16, 4221.

[18] Andjelkovic´ K., Ivanovic´ I., Niketic´ S.R., Prelesnik B. and Leovac V. M. Synthesis and structure of aqua 2'-(2,6-pyridindiylidiethylidine)- di oxamohydrazide copper(II) hydrate. *Polyhedron.* **1997**, *16*, 4221-4228.

[19] Suvarapu, L. N.; Seo, Y. K.; Baek, S. O.; Ammireddy, V. R. *J. Chem.* **2012**, *9*, 288.

[20] Bacchi, A.; Pelizzi, G.; Jeremic, D.; Sladic, D.; Gruden-Pavdvic, M.; Ardjelkovic, K. Synthesis and structural characterization of Cu(II) complexes with 2'-[1-pyridinyl]oxalohydrazide ligand. *Transition Met. Chem.* **2003**, *28*, 935-945.

[21] El-Asmy, A. A.; El-Gammal, O.A.; El-Morsey, F. E. Synthesis, Characterization, Molecular modeling and antibacterial activity of N1,N2-Bis(1-(pyridin-2-yl)ethylidene)oxalohydrazide and its Metal Complexes. *J. Mol. Struct.* **2011**, *998*, 20.

[22] Geary, W. The use of conductivity measurements in organic solvents for the characterization of coordination compounds. *J. Coord. Chem. Rev.* **1971**, *7*, 81-122.

[23] Nishkimi, M.; Appaji, N.; Yagi, K. The occurrence of superoxide anion in the reaction of reduced phenazine methosulphate and mplecular oxygen. *Biochem. Biophys. Res. Commun.* **1972**, *46(2)*, 849-854.

[24] HyperChem version 8.0 Hypercube, Inc.

[25] El-Gammal, O. A. Synthesis, characterization, molecular modeling and antimicrobial activity of 2-(2-(ethylcarbamothioyl)hydrazinyl)-2-oxo-N-phenylacetamide copper complexes. Spectrochim. Acta 2010, 75(A), 533-542.

[26] Alpert, N. L.; Keiser, W. E.; Szmanski, H. A Theory and Practice of Infrared Spectroscopy, Plenum Press, New York, 1970.

[27] Al-Hazmi, G. A.; El-Asmy, A. A. Synthesis, spectroscopy and thermal analysis of copper(II) hydrazone complexes. *J. Coord. Chem.* **2009**, *62*, 337.

[28] Sreeja, P. B.; Kurup, M. R. P.; Kishore, A.; Jasmin, C. Spectral characterization, X-ray structure and biological investigations of copper(II) ternary complexes of 2-hydroxyacetophenone 4-hydroxybenzoic acid hydrazone and heterocyclic bases. *Polyhedron* **2004**, *23*, 575-584.

[29] El-Asmy, A. A.; Al-Abdeen, A. Z.; Abo El-Maaty, W. M.; Mostafa, M. M. Synthesis and spectroscopic studies of 2,5-hexanedione bis(isonicotinylhydrazone) bis(isonicotinylhydrazone) and its first raw transition metal complexes. *Spectrochim. Acta* **2010**, *75(A)*, 1516.

[30] Nakamoto, K. *Infrared Spectra of Inorganic and Coordination compounds.* 3rd Edn., Wiley, New York 1970.

[31] Hamada, M. H.; El-Shafai, O.; El-Asmy, A.A. Enhancement of the catalytic Activity of [Cu2(TS)(OH)2(OAc)] using superconductor cuprate sample. *Transition Met. Chem.* **2006**, *31*, 714.

[32] EL-Asmy, A. A.; Gabr, I. M.; EL-Metwally, N. M.; Ghazy, S. E.; Abdel-Basseer, D. A. Spectroscopic, magnetic and thermal studies on complexes of Cu(II) and VO2+ with diacetrylmonoxime derivatives, A new method for extraction of Cu(II). *J. Coord. Chem.* **200**9, *61*, 3620.

[33] Bellamy, L. J. *The Infrared Spectra of Complex Molecule*, Methuen, London, 1985.

ISSN 2291-6458 (Print), ISSN 2291-6466 (Online)
Year 2013 | Volume 1 | Issue 4 | Page 277-291

[34] Sindhu Y, Athira CJ, Sujamol MS, Selwin RJ, Mohanan K, Synthesis, characterization, DNA cleavage, and antimicrobial studies of some transition metal complexes with a novel Schiff base derived from 2-aminopyrimidine. *Synth. React. Inorg. Met-Org. Nano-Met. Chem* **2013**; *43(3)*, 226-236.

[35] Anuradha, S.; Pramila, S. Anuradha, S.; Pramila, S. Synthesis, characterization and antiinflammatory effects of Cr(III), Mn(II), Fe(III) and Zn(II) complexes of diclofenac sodium. *Ind. J. Chem.* **2000**, *39A*, 874.

[36] Byun, J. C.; Han, C. H.; Park, Yu C. Cr(III)-tetraaza macrocyclic complexes containing auxiliary ligands (Part III); Synthesis and characterization of Cr(III)-isothiocyanato, -azido and -chloroacetato macrocyclic complexes. *Bull. Korean Chem. Soc.* **2005**, *26*, 1044.

[37] Price, E. R.; Wasson, J. R. J. Price, E.R.& Wasson, J.R., Complexes with sulfur and selenium donors-X chromium(III) piperidyldithiocarbamates. *Inorg. Nucl. Chem.* **197**4, *36*, 67.

[38] Rakha, T. H.; Bekheit, M.M. Mononuclear and polynuclear chelates of picolinoyldithiocarbazate. *Chem. Pharm. Bull.* **2000**, *48*, 914.

[39] Al-Shaalan, N. H. Synthesis, Characterization and biological activities of Cu(II), Co(II), Mn(II), Fe(II), and UO2(VI) complexes with a new Schife base hydrazone: o-hydroxyacetophenone-7-chloro-4-quinoline hydrazone. *Molecules* **2011**, *16*, 8629.

[40] El-Asmy, A. A.; Abdallah, M. A.; Mandour, Sh. A.; Ibrahim, K. M. Synt. React. Homometallic and heterometallic complexes of (E)-2-(E)-3-(o)butan-2-ylidene)hydrazinecarbothioamide. *Inorg. Met. Org. Nano-Met. Chem.* **2010**, *40*, 675-689.

[41] Bernalte-Garci a, A.; Lozano-Vila, A. M.; Luna-Giles, F.; Pedrero-Marin, R. Structural characterization of thizolinepyrazole ligand and its complexes with cobalt(II) and copper(II). *Polyhedron* **200**6, *25*, 1399-1407.

[42] Cotton, F. A.; Wilkinson G. *Advanced Inorganic Chemistry- A Comprehensive* 4th Ed., John Wiley and Sons, New York, 1986.

[43] Chandra, S.; Gupta, L. K. Electronic, EPR, magnetic and mass spectral studies of mono and homo-binuclear Co(II) and Cu(II) complexes with a novel macrocyclic ligand. *Spectrochim. Acta* **2005**, *62A*, 1102-1106.

[44] Coats A. W. and Redfern J. P. Kinetic parameters from thermogravimetric data. *Nature **1964**, 20*, 68.

[45] Guzara, S. H.; Jin, Q. H. Simple, Selective, and Sensitive Spectrophotometric Method for Determination of Trace Amounts of Nickel(II), Copper (II), Cobalt (II), and Iron (III) with a Novel Reagent 2-Pyridine Carboxaldehyde Isonicotinyl Hydrazone. *Chem. Res. Chin. Univ.* **2008**, *24 (2)*, 143-147.

The authors declare no conflict of interest